Computation of Electrostatic Forces on Solvated Molecules Using the Poisson-Boltzmann Equation

Michael K. Gilson,* Malcolm E. Davis,† Brock A. Luty, and J. Andrew McCammon

Department of Chemistry, University of Houston, Houston, Texas 77204-5641

Received: September 8, 1992; In Final Form: January 4, 1993

Numerical solutions of the Poisson-Boltzmann equation (PBE) have found wide application in the computation of electrostatic energies of hydrated molecules, including biological macromolecules. However, solving the PBE for electrostatic forces has proved more difficult, largely because of the challenge of computing the pressures exerted by a high dielectric aqueous solvent on the solute surface. This paper describes an accurate method for computing these forces. We begin by presenting a novel derivation of the forces acting in a system governed by the PBE. The resulting expression contains three distinct terms: the effect of electric fields on "fixed" atomic charges; the dielectric boundary pressure, which accounts for the tendency of the high dielectric solvent to displace the low dielectric solute wherever an electric field exists; and the ionic boundary pressure, which accounts for the tendency of the dissolved electrolyte to move into regions of nonzero electrostatic potential. Techniques for extracting each of these three force contributions from finite difference solutions of the PBE for a solvated molecule are then described. Tests of the methods against both analytic and numeric results demonstrate their accuracy. Finally, the electrostatic forces acting on the two members of a salt bridge in the enzyme triose phosphate isomerase are analyzed. The dielectric boundary pressures are found to make substantial contributions to the atomic forces. In fact, their neglect leads to the unphysical situation of a significant net electrostatic force on the system. In contrast, the ionic boundary forces are usually extremely weak at physiologic ionic strength.

1. Introduction

Continuum models of electrostatic interactions, based upon numerical solutions of the Poisson-Boltzmann equation (PBE), have found increasing application in the modeling of hydrated molecules, particularly biological macromolecules.[1-3] To date, they have been used chiefly in energy calculations. However, there is reason to expect that they will also be of value in molecular mechanics calculations, such as molecular dynamics simulations and energy minimizations. This is chiefly because the PBE approach promises to permit a simplified treatment of solvent electrostatic effects. In molecular mechanics calculations, computational limitations frequently make it difficult to include more than a few layers of solvent around a macromolecule. Including a dissolved electrolyte explicitly further increases the computational cost. Continuum models could provide a computationally efficient, albeit approximate, means of incorporating the electrostatic effects of an aqueous solvent containing dissolved ions into macromolecular simulations. There would be no question of convergence of the solvent dielectric properties, because the PBE approach yields what are essentially potentials of mean force. This fact also implies that molecular mechanics calculations using a PBE treatment of electrostatics cannot be expected to yield accurate results for fluctuations, but the results for equilibrium properties should be reasonable.

However, if the PBE is to be used in molecular mechanics calculations, methods must be devised for using the Poisson-Boltzmann equation to compute electrostatic forces, rather than energies. In doing so, it is important to recognize that the electrostatic force on an atom in a system governed by the PBE is not simply the electrostatic field, E, at the atom multiplied by the atomic charge, q. As will be discussed below in detail, such "qE forces" represent only one of three force components in the system. For now, however, the fact that something is missing may be highlighted by considering the case of a spherical centrosymmetric ion, or Born ion, in water. It is well-known that increasing the radius of the ion weakens the favorable interaction with the surrounding solvent. There must, accordingly, be a pressure acting at the boundary between the ion and the solvent. However, by symmetry, the field at the central charge is zero. Thus, the boundary pressure cannot be obtained from the qE force term. A more dramatic example is that of a hydrated spherical ion containing an eccentric charge. In this case, qE is nonzero, because the charge is attracted to the portion of the dielectric boundary to which it is closest. A molecular mechanics calculation including only the qE force would predict that the ion would translate continuously through solution; the violation of Newton's third law results from the fact that the dielectric boundary pressure has been neglected. By a similar argument, it is evident that any dissolved ions in solution also exert a pressure at the ion-exclusion boundary. As demonstrated below, the dielectric boundary pressures are far from negligible. Thus, any method for incorporating the PBE into molecular mechanics calculations must in some way account for this additional force term.

The problem of computing forces within the context of the PBE has been addressed in several ways to date. Three approaches based upon the finite difference method have been reported.

The "virtual work" method[4] is, in a sense, the most definitive. Here the electrostatic energy, G, is recalculated for small displacements d of each atom in the x, y, and z directions. The force is then just $-\Delta G/d$ for each direction. The drawback of this approach, however, is that four full finite difference calculations are required in order to calculate the force on each atom in the system.

In the DIEMOND method,[5] the emphasis is on computing the reaction field produced by the solvent. This is added to the field produced by the atomic charges in the absence of any solvent screening (which we will term the Coulombic field), to yield a net, solvent-screened, field at each atomic charge. Force is then computed as charge times field ("qE" force). The problem of solvent pressure is dealt with primarily by what may be termed the surface charge approximation,[4] where the pressure on a

† Current address: Macromolecular Modeling, Bristol-Myers Squibb, P.O. Box 4000, Princeton, NJ 08543-4000.

0022-3654/93/2097-3591$04.00/0

dielectric boundary is calculated as σE, where σ is surface charge density, and E is the electrostatic field, or some variant thereof, at the boundary. Although this approximation can be made to yield zero net force on the system, satisfying Newton's third law, it is in fact approximate and can be shown to yield incorrect solvation energies. For example, when this approximation is used to calculate the charge–solvent interaction energy of a Born ion as an integral of force-distance, as the ion radius is contracted from infinity to the ionic radius, the result is in error by a factor of two.

A more recent paper describes molecular dynamics simulations of bovine pancreatic trypsin inhibitor, in which the finite difference method is used to compute the solvent reaction field at each charged atom, and the net field at each atom is written as the sum of this reaction field and the Coulombic field due to the other atoms.[6] These calculations neglect dielectric boundary pressures. As a consequence, there is no guarantee that Newton's third law will be obeyed. Despite this approximation, the trajectories do appear to be remarkably well-behaved.

Another promising approach to the incorporation of PBE electrostatics into molecular mechanics is based upon the use of the boundary element technique.[7-11] Because this method includes an explicit dielectric boundary surface, it is conceptually straightforward to compute boundary pressures using the Maxwell stress tensor. Such an approach is described by Zauhar,[12] who includes both qE forces and boundary pressures in an energy minimization of a zwitterionic tripeptide. It should be noted, however, that the accuracy of the boundary pressures computed by this technique have not yet been demonstrated. Another issue which must be addressed is the treatment of "reentrant surface",[13] in cases where the dielectric boundary is defined in terms of the probe accessible surface. For example, the boundary pressure acting on reentrant surface must be transduced properly into the forces on actual atoms. The problems with defining the dielectric boundary to be the probe-accessible surface are further discussed below.

The methods so far discussed all require that the PBE be solved repeatedly during a molecular mechanics calculation. This is a computationally intensive approach, and as a consequence simplified methods for incorporating continuum electrostatics into molecular simulations have been proposed. One such involves the use of the generalized Born equation, together with an empirical interaction function involving charge–charge distances and effective radii.[14] This method appears to be well suited for simulations of small molecules in solution, where the effective radii are not expected to vary much during the simulation. However, the function does not permit the calculation of derivatives with respect to effective radius. As a consequence, there is no force opposing the desolvation of charged atoms, so this method should probably be used with caution in macromolecular simulations where changes in solvation may be important. Another simplified method for incorporating continuum electrostatics into simulations, the "field energy method",[15] is designed to yield accurate electrostatic fields at atoms. The electrostatic forces on atoms are then taken to be charge times field (qE). Again, however, dielectric boundary forces are not included. Another method has been devised specifically for treating the charge–solvent interactions of individual atoms.[16] However, this approach in effect distributes dielectric boundary forces over all atoms in a solute, rather than associating them solely with atoms which contribute to the dielectric boundary. Finally, a number of screening functions for charge–charge interactions have been developed, starting with the simple distance-dependent dielectric constant ($\epsilon = r$); to alternative forms where $\epsilon = \alpha r$, α being a proportionality constant;[17,18] to distance-dependent screening functions having more complicated functional forms.[19-21] Although such functions may be quite successful for computing the interactions of groups on the surface of a protein, their ability to reproduce the results of the PBE is obviously limited.

To sum up, it would appear that, aside from the laborious virtual work method, no numerical method of demonstrated accuracy currently exists for computing the electrostatic forces on atoms predicted by the PBE. The present work describes a novel method for computing these forces, using finite difference solutions of the PBE. The structure of the paper is as follows. The Methods section begins with a variational derivation of a complete force expression for the PBE equation. This derivation extends the line of reasoning used in recent variational derivations of the free energy expression for the PBE.[22,23] When written as a force density, the resulting force expression contains three distinct terms. Although the same expression may be derived as a limiting case of the primitive electrolyte model[24] and is also explicit in the theory of the electrical double layer,[25] the present derivation is particularly straightforward. The Methods section next describes numerical methods for computing each of the three force terms. The Results section presents accuracy tests, and a sample calculation on a salt bridge of triose phosphate isomerase. Finally, the limitations and implications of this work are discussed.

2. Methods

2.1. Variational Derivation of Force Expressions. This section presents a novel variational derivation of expressions for the electrostatic forces in a system governed by the Poisson–Boltzmann equation. The system of interest is that of a macromolecule of known three-dimensional structure, having a low dielectric constant and immersed in a high dielectric solvent containing dissolved ions. The parameters of this system can be described by the "fixed" charge density, $\rho^f = \rho^f(\mathbf{r})$, associated with the atoms of the macromolecule; the permittivity, $\epsilon = \epsilon_0\epsilon_r(\mathbf{r})$, as a function of position, where ϵ_0 is the permittivity of vacuum, and ϵ_r is the relative permittivity (dielectric constant); the bulk concentration c_i of each of N ionic species i; the charge of each ionic species, q_i; and a "masking" function $\lambda = \lambda(\mathbf{r})$ which has a value of 0 wherever ions cannot penetrate and a value of 1 where they can. $\lambda(\mathbf{r})$ will thus be zero within the macromolecule and 1 elsewhere. If there is an ion-exclusion layer, or Stern layer, around the macromolecule, $\lambda(\mathbf{r})$ will be 0 there as well. In principle, the thickness of the Stern layer will depend upon the radius of the ionic species. Therefore, each ionic species i should have its own $\lambda_i(\mathbf{r})$. For simplicity, however, we assume here that a single $\lambda(\mathbf{r})$ provides an adequate description of the ion-exclusion volume.

We begin with an expression which has been shown[22,23] to represent a free energy functional for the Poisson–Boltzmann equation. The present form permits consideration of an asymmetric electrolyte, and is given in SI units:

$$G(\phi,\rho^f,\epsilon,\lambda) = \int_V (\rho^f\phi - {}^1/_2\epsilon\nabla\phi\cdot\nabla\phi - kT\sum_i^N [c_i(e^{-q_i\phi/kT} - 1)]\lambda)\, dV \quad (1)$$

where $\phi = \phi(\mathbf{r})$ is the electrostatic potential as a function of position, k is Boltzmann's constant, and T is the absolute temperature. The integral is taken over all space. The variations in the functions ρ^f, ϵ, ϕ, and λ are related to variations in this functional by

$$\delta G = \int_V (\phi\delta\rho^f - {}^1/_2\nabla\phi\cdot\nabla\phi\delta\epsilon - kT\sum_i^N [(e^{-q_i\phi/kT} - 1)c_i]\,\delta\lambda + \rho^f\delta\phi - \epsilon\nabla\phi\cdot\nabla(\delta\phi) + \lambda\sum_i^N q_i c_i e^{-q_i\phi/kT}\delta\phi)\, dV \quad (2)$$

Integrating the fifth term by parts

$$\int_V(\epsilon\nabla\phi)\cdot(\nabla\delta\phi)\,dV = \int_V\nabla\cdot(\epsilon\delta\phi\nabla\phi)\,dV - \int_V(\delta\phi)\nabla\cdot(\epsilon\nabla\phi)\,dV \quad (3)$$

and using the divergence theorem to convert the first integral on the right-hand side into a vanishing surface integral at infinity allows us to rewrite the functional as

$$\delta G = \int_V(\phi\delta\rho^f - {}^1/_2\nabla\phi\cdot\nabla\phi\delta\epsilon - kT\sum_i^N[(e^{-q_i\phi/kT}-1)c_i]\delta\lambda + \{\rho^f + \nabla\cdot(\epsilon\nabla\phi) + \lambda\sum_i^N q_ic_ie^{-q_i\phi/kT}\}\delta\phi)\,dV \quad (4)$$

For a given system $\delta\rho^f = \delta\epsilon = \delta\lambda = 0$), we wish to find the function $\phi(\mathbf{r})$ which extremizes G. Thus $\delta G = 0$ for any small arbitrary $\delta\phi$. This condition is met when the term in braces vanishes, or

$$-\nabla\cdot(\epsilon\nabla\phi) = \rho^f + \lambda\sum_i^N q_ic_ie^{-q_i\phi/kT} \quad (5)$$

which is the Poisson–Boltzmann equation. Here the right-hand side represents the sum of the fixed charge ρ^f of the solute, and the induced ("mobile") space charge in the solvent. This result confirms that the potential which extremizes G is also the potential which satisfies the Poisson–Boltzmann equation.[22,23]

It is now possible to write the variation of G with the three spatially varying parameters ρ^f, ϵ, and λ, as

$$\delta G = \int_V(\phi\delta\rho^f - {}^1/_2E^2\delta\epsilon - kT\sum_i^N[(e^{-q_i\phi/kT}-1)c_i]\delta\lambda)\,dV \quad (6)$$

where E is the electrostatic field strength.

A force density $\mathbf{f}(\mathbf{r})$ is defined, such that

$$-\delta G = \int_V\mathbf{f}(\mathbf{r})\cdot\mathbf{s}(\mathbf{r})\,dV \quad (7)$$

where $\mathbf{s}(\mathbf{r})$ is some arbitrary infinitesimal displacement of the system.[26] To convert eq 6 to the form of eq 7, it is necessary to express $\delta\rho^f$, $\delta\epsilon$, and $\delta\lambda$ in terms of s. Because ρ^f is a true charge density

$$\delta\rho^f = -\nabla\cdot(\rho^f\mathbf{s}) \quad (8)$$

This expression, which follows from conservation of charge,[26] permits the first integral of eq 6 to be rewritten as

$$\begin{aligned}\int_V\phi\delta\rho^f dV &= -\int_V\phi\nabla\cdot(\rho^f\mathbf{s})\,dV \\ &= -\int_V\nabla\cdot(\phi\rho^f\mathbf{s})\,dV + \int_V\rho^f\mathbf{s}\cdot\nabla\phi\,dV \\ &= -\int_V\mathbf{s}\cdot(\rho^f\mathbf{E})\,dV \end{aligned} \quad (9)$$

where the divergence theorem has been used to convert the integral of $\nabla\cdot(\phi\rho^f\mathbf{s})$ to a vanishing integral over a surface at an infinite distance. $\mathbf{E}$ is the electrostatic field vector.

For ϵ and λ, we write[27]

$$\delta\epsilon = -\mathbf{s}\cdot\nabla\epsilon + \frac{\partial\epsilon}{\partial\tau}d\tau$$

$$\delta\lambda = -\mathbf{s}\cdot\nabla\lambda + \frac{\partial\lambda}{\partial\tau}d\tau \quad (10)$$

where τ is the mass density of the medium as a function of position. Continuum models for electrostatic interactions in macromolecules typically assume that ϵ and λ are independent of density. For this reason, and in the interest of simplicity, we here neglect the density dependent terms in the expression for $\delta\epsilon$ and $\delta\lambda$. However, these terms can readily be included and carried through the following derivation, leading to their appearance in the stress tensor. The classical Maxwell stress tensor in fact includes the density-dependent term in ϵ, which is associated with electrostrictive effects.[26]

Substituting the resulting expressions for $\delta\rho^f$, $\delta\epsilon$, and $\delta\lambda$ into eq 6 and rewriting in the form of eq 7 yields

$$-\delta G = \int_V\mathbf{s}\cdot\{\rho^f\mathbf{E} - {}^1/_2E^2\nabla\epsilon - kT\sum_i^N[(e^{-q_i\phi/kT}-1)c_i]\nabla\lambda\}\,dV \quad (11)$$

where the expression in braces is the desired force density $\mathbf{f}$.

The first term in the force density yields the usual interactions of fixed charges with the electrical field ("qE" force), which may be partitioned into the Coulomb's law fields of atomic charges in the dielectric constant of the molecular interior, plus the reaction field due to the solvent around the molecule. The second term yields the forces acting at boundaries between different dielectric media. The last term yields the forces acting at the ion-exclusion boundary, which delineates the region into which mobile solvent ions cannot penetrate. The two boundary forces will always be directed normal to the boundaries, because they are proportional to the gradients of ϵ and λ. The first two terms in this force density expression are included in the force density expression of classical electrostatics.[27] The present expression differs from the classical force density in neglecting the density dependence of the dielectric constant and in including the ionic term.

Essentially the same derivation can be used to obtain a force density expression in the context of the linearized Poisson–Boltzmann equation. The linearizing approximation is made in eq 1, where the Taylor series expansion for the exponential is used:

$$-kT\sum_i^N[c_i(e^{-q_i\phi/kT}-1)]\lambda \approx \left[\phi\sum_i^N c_iq_i - \frac{\phi^2}{2kT}\sum_i^N c_iq_i^2\right]\lambda \quad (12)$$

The first sum vanishes because of electroneutrality, leaving

$$-kT\sum_i^N[c_i(e^{-q_i\phi/kT}-1)]\lambda \approx -{}^1/_2\epsilon\kappa^2\phi^2\lambda \quad (13)$$

where κ is the usual Debye–Huckel parameter:

$$\kappa^2 = \frac{1}{\epsilon kT}\sum_i^N c_iq_i^2 \quad (14)$$

The resulting force density is

$$\mathbf{f} = \rho^f\mathbf{E} - {}^1/_2E^2\nabla\epsilon - {}^1/_2\epsilon\kappa^2\phi^2\nabla\lambda \quad (15)$$

This force density expression is readily convertible into a tensor form, identical to the standard Maxwell stress tensor, except for the fact that the diagonal elements have an additional term which accounts for the ionic pressure. This is consistent with the contact theorem of Henderson et al.[28,29]

2.2. Numerical Implementation. From the above derivation, it can be seen that computing the electrostatic forces in a system governed by the PBE actually requires solving for three different terms: the ρ^fE term, which corresponds to the qE term discussed in the Introduction; the dielectric pressure term $-{}^1/_2E^2\nabla\epsilon$; and the ionic pressure term, $-kT\sum_i^N[(e^{-q_i\phi/kT}-1)c_i]\nabla\lambda$. In a molecular system, we will usually be interested in computing the electrostatic force acting on each atom. For an atom which does not form part of a dielectric or ionic boundary, the force will be given by just the qE term. However, any atom which forms part of a boundary will feel additional boundary pressures, which must

be summed with the qE term to give the net force on the atom. The three sections which follow describe how each of the three force contributions may be computed from a finite difference solution to the Poisson–Boltzmann equation.

2.2.1. Forces on Free Charges. The qE forces are calculated as follows.[4,6] A finite difference calculation of the full system is performed, yielding a potential distribution ϕ^{I}. A second calculation is then performed with the solvent region now set to the dielectric constant of the solute and zero ionic strength, yielding ϕ^{II}. The latter is an approximation to the Coulomb's law potential, but it may contain significant errors for charges which are close together, due to the discrete nature of the finite difference grid. However, as discussed previously[4,6] and again demonstrated below, numerical experiments show that $\phi^{I} - \phi^{II}$ can be an accurate representation of the reaction potential generated by the solvent, and the gradient of this reaction potential can be an accurate reaction field.

When implemented in this fashion, the method requires that two finite difference calculations be performed. In fact, the second calculation is not needed. Consider the potential at some atomic charge. The finite difference grid yields accurate Coulomb's law potentials for atomic charges which are more than perhaps 10 grid units apart. The contribution of closer charges to the grid field may be computed rapidly using the appropriate Green's function for the finite difference grid with a uniform permittivity equal to that of the solute interior.[30] This may be subtracted from ϕ^{I}, and the correct Coulomb's law field added back in its place. This procedure can yield accurate qE forces without the need to perform a second finite difference grid calculation.

2.2.2. Dielectric Boundary Forces. Computing the dielectric boundary forces accurately presents a considerable numerical challenge. In principle, boundary forces may be computed in terms of either the force density formulation given above or alternatively in terms of the tensor formulation given in Appendix A. The latter involves the evaluation of surface integrals. As a consequence, it is probably the best formulation to use when the boundary element method is used to solve the PBE. On the other hand, because the finite difference method yields particularly inaccurate electrostatic fields at the dielectric boundary, it is not well suited to a straightforward application of the tensor method. What does appear to be feasible is to place surfaces of integration approximately one grid spacing within and without the boundary and to apply the tensor formulation on these surfaces.[31] Work on this method is in progress. However, in the present paper, a force density method is described. As shown below, this formulation is particularly well suited to the finite difference method.

Equation 6 shows that the change in electrostatic energy with a variation in ϵ is

$$\delta G = -\int {}^{1}/_{2} E^{2} \delta\epsilon \tag{16}$$

If $\delta\epsilon$ is the consequence of a small movement Δx of an atom along the x axis, say, then the x component of the dielectric boundary force on this atom will be $-\Delta G/\Delta x$. The other force components can be written similarly.

To implement this basic idea numerically, it is necessary to use the appropriate grid definitions of E and ϵ. Because the dielectric pressure term comes from the second term of the energy density expression (eq 1), the appropriate discretization of the dielectric boundary pressure term must be based upon the discretization of this component of the energy density, which is

$$G = -\sum_{ijk} (h^{3}/6)[\epsilon_{x}(i,j,k)(\phi(i+1,j,k) - \phi(i,j,k))^{2} + \epsilon_{y}(i,j,k)(\phi(i,j+1,k) - \phi(i,j,k))^{2} + \epsilon_{z}(i,j,k)(\phi(i,j,k+1) - \phi(i,j,k))^{2}] \tag{17}$$

where h is the grid spacing in angstroms; $\epsilon_{x}(i,j,k)$, $\epsilon_{y}(i,j,k)$, and $\epsilon_{z}(i,j,k)$ are the permittivities associated with the x-, y-, and z-directions grid branches originating at grid point (i,j,k); and $\phi(i,j,k)$ is the potential at grid point (i,j,k). Therefore, the x component of the dielectric boundary force on an atom will be

$$F_{x} = \frac{h^{3}}{6}\sum_{ijk}\left[\frac{\partial\epsilon_{x}(i,j,k)}{\partial x}(\phi(i+1,j,k) - \phi(i,j,k))^{2} + \frac{\partial\epsilon_{y}(i,j,k)}{\partial x}(\phi(i,j+1,k) - \phi(i,j,k))^{2} + \frac{\partial\epsilon_{z}(i,j,k)}{\partial x}(\phi(i,j,k+1) - \phi(i,j,k))^{2}\right] \tag{18}$$

where the partial derivatives are taken with respect to atomic coordinates. Similar expressions will apply for the y- and z-force components.

When dielectric boundary smoothing is used[32] and when the dielectric boundary is defined as the van der Waals surface of the solute, the only grid branches whose permittivities will be affected by infinitesimal atomic motions are the "fractional" grid branches, which are only partially covered by atoms, and therefore form the dielectric boundary. In the current implementation of the smoothing algorithm, the permittivity of a grid branch is given by

$$\epsilon = \frac{\epsilon_{i}\epsilon_{s}}{(\epsilon_{i} + \min(1, a_{n} + a_{p})(\epsilon_{s} - \epsilon_{i}))} \tag{19}$$

where ϵ_{i} and ϵ_{s} are the solute and solvent permittivities, respectively; a_{n} is the largest fraction of the grid branch internal to any atom whose surface intersects the grid branch once from the negative direction; a_{p} is the largest fraction of the grid branch internal to any atom whose surface intersects the grid branch once from the positive direction; and the min function limits the internal fraction of the grid branch to a maximum of 1. The permittivity of a grid branch which is intersected twice by the surface of a single atom is set to ϵ_{i}. This permits the use of a fast algorithm and also avoids the occurrence of a singularity in the force calculations—see below. Note that a maximum of two atoms (the ones associated with a_{n} and a_{p}) are involved in determining the permittivity of a fractional branch.

The contribution of an x-directed fractional grid branch to the force on an atom which sets a_{n} (i.e., which intersects the branch from the negative direction) will be

$$\mathbf{f} = \frac{h^{3}}{6}(\phi(i+1,j,k) - \phi(i,j,k))^{2}\frac{\partial\epsilon}{\partial a_{n}}\left(\hat{\mathbf{x}}\frac{\partial a_{n}}{\partial x} + \hat{\mathbf{y}}\frac{\partial a_{n}}{\partial y} + \hat{\mathbf{z}}\frac{\partial a_{n}}{\partial z}\right) \tag{20}$$

Substitution of a_{p} for a_{n} yields the result for an atom which sets a_{p}. It can be shown that

$$\frac{\partial a_{n}}{\partial x} = -\frac{\partial a_{p}}{\partial x} = \frac{1}{h} \tag{21a}$$

$$\frac{\partial a_{n}}{\partial y} = \frac{\partial a_{p}}{\partial y} = \frac{\Delta y}{h\Delta x} \tag{21b}$$

$$\frac{\partial a_{n}}{\partial z} = \frac{\partial a_{p}}{\partial z} = \frac{\Delta z}{h\Delta x} \tag{21c}$$

where Δx, Δy, and Δz are the x, y, and z distances between the atomic center and point where the atom intersects the grid branch. (The actual algorithm is simplified by approximating these as

distances to the grid branch center.) Equation 20 becomes

$$\mathbf{f} = \mathbf{r}\frac{h^2}{6}\frac{\epsilon^2(\epsilon_s - \epsilon_i)}{\epsilon_i\epsilon_s\Delta x}(\phi(i+1,j,k) - \phi(i,j,k))^2 \qquad (22)$$

where $\mathbf{r}$ isi the vector pointing from the grid branch center to the atom center.

Examination of the previous equation reveals that an infinite force will occur if $\Delta x = 0$. In practice, however, this does not arise. This is because, as noted above, we measure Δx from the center of the grid branch, rather than from the intersection point. Therefore, any atom which intersects the branch with $\Delta x = 0$, will intersect the branch twice. In this case, ϵ is set directly to ϵ_i, and the branch will not be a force-generating, fractional grid branch.

A related approach is used in computing atomic forces when the probe-accessible boundary definition[13] is used. The procedure is based upon the method of generating the probe-accessible dielectric map, which has been described previously.[33] Briefly, however, all grid branches are initially set to ϵ_s. Then the radius of each atom is enlarged by the radius of the probe sphere, and all grid branches whose centers lie within an enlarged atom have their permittivity set to ϵ_i. Next, a set of points on the Lee and Richards[34] surface is generated. These points represent possible locations of the center of a probe molecule and lie one probe radius off the atomic van der Waals surfaces. Finally, a hypothetical probe sphere is placed at each of these surface points, and the contents of each sphere is set back to ϵ_s. Dielectric boundary smoothing is incorporated into the last step: any grid branch intersected by the surface of a probe sphere is assigned a permittivity intermediate between ϵ_i and ϵ_s, using the formula given above, except that ϵ_i and ϵ_s are interchanged. Thus, the larger the fraction of a grid branch covered by one or two probe spheres, the closer to ϵ_s will be the branch's permittivity. Note that a grid branch which is set to a fractional permittivity by one probe sphere may turn out to fall completely inside another. In this case, its permittivity is set to that of the solvent, and it is not treated as a force-generating fractional branch.

The key to the treatment of forces on probe-accessible surfaces is to calculate the force on each of the hypothetical probe spheres, using the same formulas as given above for forces on van der Waals atom spheres. We find that the total boundary force in the system is given quite accurately by the net boundary force on all the probe spheres. The next step is to convert from forces on hypothetical probe spheres to forces on atoms.

In principle, the force on a probe sphere will be applied to all the atoms which it contacts. The simplest case, then, is that of a probe sphere which contacts only one atom (a "contact" probe sphere). Here the force is transmitted simply along the line of centers of the atom and probe sphere, which will be very similar to the atom's surface normal. Therefore, it is appropriate simply to add the force contributions of such probe spheres to the net boundary forces on the atoms which they contact.

The case of "reentrant" probe spheres—those probe spheres which contact two atoms simultaneously and which therefore are associated with toroidal reentrant surface—is treated as follows. The first problem is to identify such spheres. The probe sphere points on the Lee and Richards surface are established by generating a set of hundreds or thousands of points on a sphere around each atom i, having the radius of the atom i plus that of the probe sphere. Any such point which is closer than atom radius (r_j) plus probe radius to another atom j is deleted from the list, leaving a list of accepted probe sphere locations. Each of these remaining points still "belongs", in a sense, to the atom i. A reentrant probe sphere may be distinguished from a contact probe sphere by the fact that it contributes to a surface region further than r_i from the center of atom i. In practice, any probe sphere which creates one or more fractional grid branches whose centers are greater than $r_i + 1.1h/2$ from the center of atom i is determined to be a reentrant sphere. (Adding $h/2$ accounts for the fact that a grid branch can be fractional if a probe sphere intersects it anywhere along its length. The factor of 1.1 is a somewhat arbitrary selected adjustment for the fact that a contact probe sphere may actually create a fractional grid branch slightly greater than $r_i + h/2$ from the center of its atom i, because of the finite number of probe locations.) Recalling that a reentrant probe sphere actually contacts two atoms, it is necessary to identify these two atoms so that the force on this probe sphere can be appropriately distributed between them. One of the atoms is that to which the probe sphere "belongs", atom i. We take the other atom to be that surface atom j which is closest to the probe sphere (after subtracting the radius of atom j). The search for such atoms is made rapid by means of a neighbor list.

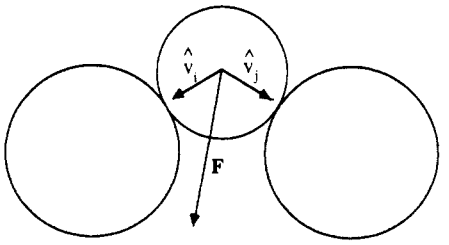

Figure 1. Distribution of the force on a reentrant probe sphere between the two atoms it contacts. Two atomic van der Waals spheres (shaded) are shown, together with a reentrant probe sphere. Vectors designate the dielectric boundary force, F, on the probe sphere, and the unit vectors, $\hat{v}_i$ and $\hat{v}_j$, pointing from the probe to the two atoms, i and j.

Although the dielectric boundary pressure on a patch of reentrant surface must be normal to the surface and therefore may initially appear not to affect the atoms which are associated with it, in fact pressure on reentrant surface tends to separate the atoms. This is because increasing the separation of the atoms allows the reentrant surface to move inward. Therefore, pressure on the reentrant surface drives the atoms apart. One way of relating force on reentrant surface to atom forces is illustrated in Figure 1. The total force $\mathbf{F}$ on each reentrant probe sphere is computed, and distributed between the two atoms i and j in such a way that the force on each atom, $\mathbf{f}_i$ and $\mathbf{f}_j$ is directed along the line joining the probe sphere and atom sphere centers, with the requirement that $\mathbf{F} = \mathbf{f}_i + \mathbf{f}_j$. Thus

$$\mathbf{f}_j = \hat{v}_j\left(\frac{\hat{v}_i\cdot\mathbf{F} - (\hat{v}_i\cdot\mathbf{F})(\hat{v}_i\cdot\hat{v}_i)}{1 - \hat{v}_i\cdot\hat{v}_j}\right)$$

$$\mathbf{f}_i = \hat{v}_i(\hat{v}_i\cdot\mathbf{F} - \mathbf{f}_j(\hat{v}_i\cdot\hat{v}_j)) \qquad (23)$$

where $\hat{v}_i$ and $\hat{v}_j$ are unit vectors pointing from the probe sphere toward atoms i and j, respectively.

In this way, each probe sphere which determines either a_n or a_p for a fractional grid branch contributes to atomic forces, either by simple summation if the sphere contacts only one atom, or by eq 24 if it is associated with reentrant surface. It is possible for a probe sphere to contact three or even more atoms at a time. The present algorithm does not address this level of complexity. However, it seems likely that treating such cases approximately, as described here, will not substantially alter the results. This issue is examined in at least a preliminary way, in the Results section.

2.2.3. Ionic Boundary Forces. The ionic boundary forces are considerably easier to calculate than are the dielectric boundary forces. From eq 11, the ionic boundary force equals a constant times $\nabla\lambda$. Since λ is a unit step function at the ionic boundary, its gradient is a delta function along the surface normal. Therefore, an integral of the ionic force density term of eq 11 from inside to outside the boundary, along the normal, yields a

TABLE I: Analytic versus Numerical Forces (kcal/(mol Å)) versus Distance (Å) for a 0.5 Proton Point-Charge in the Vicinity of a 1.5-Å Neutral Cavity[a]

		case A		case B		case C		case D	
dist (Å)	analyt	QEF	DBF	QEF	DBF	QEF	DBF	QEF	DBF
3.0	0.03	0.03	−0.00	0.03	−0.01	0.03	−0.02	0.03	0.00
2.8	0.04	0.05	−0.00	0.05	−0.02	0.04	−0.03	0.04	0.00
2.6	0.06	0.08	−0.01	0.08	−0.03	0.07	−0.06	0.07	−0.01
2.4	0.12	0.14	−0.02	0.16	−0.04	0.13	−0.10	0.13	−0.02
2.2	0.23	0.29	−0.04	0.36	−0.08	0.27	−0.17	0.27	−0.05
2.0	0.56	0.67	−0.06	1.15	−0.16	0.66	−0.33	0.72	−0.15
1.8	1.94	1.96	−0.12	4.70	−0.41	2.44	−0.62	2.87	−0.67
1.6	22.24	2.10	−0.22	284.20	−165.44	14.77	−1.67	80.56	−129.62
1.4	2024.30	323.12	−292.64	392.35	−1848.41	337.50	−383.74	448.10	−1899.10
1.2	222.79	190.79	−225.22	292.46	−252.10	224.08	−244.43	198.44	−209.42
1.0	78.05	82.95	−79.76	84.84	−81.37	76.92	−77.99	77.58	−77.05
0.8	37.67	37.78	−38.11	38.77	−38.45	37.62	−37.57	37.54	−37.44
0.6	20.51	20.83	−20.67	20.74	−20.81	20.51	−20.28	20.54	−20.54
0.4	11.19	11.29	−11.25	11.26	−11.34	11.20	−11.03	11.20	−11.20
0.2	5.00	5.03	−5.02	5.04	−5.07	5.00	−4.92	5.00	−4.99

[a] Second column: analytic result. Cases A, B, C, and D: direct force calculations for four different orientations and positions on the finite difference grid (see text). QEF: charge-reaction field force on the point charge. DBF: dielectric boundary force.

boundary force per unit area of

$$dF/dA = -\hat{n}kT\sum_{i}^{N}[(e^{-q_i\phi/kT} - 1)c_i] \qquad (24)$$

where $\hat{n}$ is the outward surface normal. What makes the calculation easy numerically is that neither the electrostatic potential nor the field are discontinuous at the ionic boundary, unless this boundary happens to coincide with the dielectric boundary. Therefore, as long as a Stern layer whose thickness is one or more grid spacings is used, the ionic boundary will be sufficiently far from the dielectric boundary that the ion-boundary potentials will be accurate. As a consequence, the ionic pressure, which depends directly upon potential, will be accurate.

In practice, these forces are readily calculated by spreading an even distribution of surface points over the ionic boundary, and computing the ionic force at each point. Since the ionic boundary is customarily treated as the locus of points accessible to the *center* of an ion-sized probe sphere, each surface point is clearly associated with a solute atom, and the ionic force on each atom is obtained by summing the force associated with each of its surface points.

2.3. Accuracy Tests. The Results section presents a series of accuracy tests for the methods just described. The parameters and software used in these computations are as follows. Except as otherwise specified, all finite difference Poisson–Boltzmann (FDPB) calculations use a 58 × 58 × 58 grid with grid spacing 0.21 Å, internal dielectric constant 1, external dielectric constant 80, and ionic strength 0. Probe-accessible dielectric maps are calculated using a probe of radius 1.4 Å and approximately 4000 initial probe sphere locations per atom (see above). Grid boundary potentials are set using Coulomb's law for all fixed charges in the system, with the solvent dielectric constant, and Debye–Huckel ionic screening if the ionic strength is not zero. Although the methods described here are in principle valid for both the linearized and the nonlinear PBE, the present calculations are limited to the linearized case. The calculations are performed with a modified version of the program UHBD.[35]

The calculation on triose phosphate isomerase is based upon the Protein Data Bank[36] file 1TIM.[37] Polar hydrogens are placed using the program CHARMM[38] without altering the coordinates of non-hydrogen atoms. The atomic charges are those of OPLS[39] and the radii those of MIDAS.[40]

3. Results

3.1. Accuracy of Numerical Methods. *3.1.1. Analytic Test of QE and Dielectric Boundary Forces.* The first test case is one for which an analytic expression is available. A point charge of +0.5 proton charges is moved from the solvent into a 1.5-Å spherical low dielectric cavity in 0.2-Å steps, starting at a distance of 3.0 Å from the center of the cavity. The ionic strength is zero. To assess the stability of the results as the system is moved about the dielectric grid, four separate runs are performed. In the first two, the line joining the cavity and the charge lies on the x axis, while in the second two, it lies along the (1,1,1) vector from the center of the neutral sphere. In the first and third, the center of the grid coincides with the center of the neutral cavity, and in the second and fourth the grid center is offset from the cavity center by 0.1 Å (≈one-half grid branch) along each axis. These calculations use the van der Waals surface definition, as described in Methods. Table I compares both the qE and dielectric boundary force results of these four calculations with the analytic results. The forces presented are the components along the axes joining the charge and the origin; other force components are negligible. Note that the forces on the cavity and the point charge should be equal and opposite, and equal in magnitude to the analytic force on the charge.

Recalling that the dielectric boundary is at 1.5 Å and that the grid spacing is 0.21 Å, the qE forces are quite accurate when the charge is greater than 3–4 grid spacings away from the boundary. The dielectric boundary forces are not particularly accurate when the charge is outside the cavity. However, the results are remarkably accurate when the charge is inside the cavity. In fact, the boundary forces agree with the analytic result somewhat better than do the qE forces, especially at the 1.0-Å distance. Although one might wish for better results for the case where the charge is outside the sphere, the inaccuracy need not be particularly problematic because the forces are weak in any case. By the same token, the accuracy of the forces for the internal charge is encouraging, because these forces are quite strong. It should also be noted that in most practical calculations, every point charge will be at least 1.0 Å away from any dielectric boundary, because point charges are placed at atom centers.

3.1.2. Analytic Test of QE and Ionic Boundary Forces. Analytic expressions are also available for electrostatic potentials in the case of a point charge inside a spherical ion-excluding region surrounded by an electrolyte described by the linearized PBE,[41] when the internal and external dielectric constants are equal. Forces for this case may therefore be obtained by numerical differentiation. Table II presents comparisons of such "semi-analytic" forces with ionic boundary forces computed as described in Methods. The charge is located 0–1.3 Å from the center of a 2.5-Å radius ion-excluding sphere in a 150 mM electrolyte at 300 K. Calculations are performed for the same four positions and orientations relative to the finite difference grid described in the previous section. Note that in this two atom system, the

TABLE II: "Semianalytic" versus Numerical Forces (kcal/(mol Å)) as a Function of Distance Å for a 0.5 Proton Point Charge in the Vicinity of a 2.5-Å Ion-Exclusion Sphere[a]

		case A		case B		case C		case D	
dist (Å)	analyt	QEF	IBF	QEF	IBF	QEF	IBF	QEF	IBF
1.3	0.248	0.250	−0.247	0.253	−0.249	0.251	−0.246	0.249	−0.247
1.2	0.223	0.225	−0.222	0.227	−0.224	0.226	−0.221	0.224	−0.222
1.1	0.200	0.202	−0.199	0.203	−0.200	0.202	−0.198	0.201	−0.198
1.0	0.178	0.180	−0.177	0.181	−0.178	0.180	−0.176	0.179	−0.177
0.9	0.157	0.159	−0.157	0.160	−0.157	0.160	−0.156	0.158	−0.156
0.8	0.138	0.140	−0.137	0.140	−0.138	0.140	−0.136	0.138	−0.137
0.7	0.119	0.121	−0.118	0.120	−0.119	0.121	−0.118	0.119	−0.118
0.6	0.101	0.102	−0.100	0.102	−0.101	0.102	−0.100	0.101	−0.100
0.5	0.083	0.084	−0.083	0.084	−0.083	0.085	−0.082	0.083	−0.082
0.4	0.066	0.067	−0.066	0.066	−0.066	0.067	−0.065	0.066	−0.065
0.3	0.049	0.050	−0.049	0.049	−0.049	0.050	−0.040	0.049	−0.049
0.2	0.033	0.033	−0.033	0.032	−0.033	0.033	−0.032	0.032	−0.032
0.1	0.016	0.017	−0.016	0.016	−0.016	0.017	−0.016	0.015	−0.016
0.0	0.000	0.000	0.000	−0.001	0.000	0.000	0.000	0.002	0.000

[a] IBF: ionic boundary force. See Table I caption for definitions of other terms. All forces in this table have been multiplied by 100.

boundary force should be equal and opposite to the qE force on the point charge. Both the numerical qE forces and the ionic boundary forces agree extremely well with the analytic results for all four orientations. Note also that the values in the table are very small, despite the fact that they have been multiplied by 100, for presentation.

Although analytic expressions for ionic forces are not available for the case where a dielectric boundary is also present, it is of interest to examine the stability of the results in such a case. When the above calculations were repeated with a low dielectric cavity of radius 1.5 Å concentric with the ion-exclusion cavity, the results for the four positions and orientations on a finite difference grid agreed with each other extremely well. The largest percentage difference between any two of these calculations is 4%. This suggests that the numerical instability at the dielectric boundary does not substantially affect the potentials computed at the Stern layer boundary 1 Å away.

Another notable result of these calculations is that the ionic boundary forces are essentially negligible in comparison with the dielectric boundary forces, especially given the numerical uncertainty associated with the latter. Therefore, in many applications it should be possible to neglect the contributions of ionic boundary forces.

3.1.3. Two Cavities: Comparison with Virtual Work Forces and Analytic Transfer Energies. The first case examined is that of the complete burial of a small charged atom in a somewhat larger neutral atom. The charged atom bears 0.5 proton charges and is surrounded by a low dielectric cavity of 1-Å radius. The neutral atom is a low dielectric cavity of radius 1.5 Å, located at the origin. The charged atom is initially placed 5.0 Å away from the origin, and is moved to the origin in steps of 0.2 Å. The overall work of the process may be estimated as $\sum_i 0.2F_i$, where i indexes the step, and F_i is the atomic force along the axis joining the two atoms. The force on the neutral atom is simply the dielectric cavity force acting on it. The force on the charged atom is the sum of its qE force and its dielectric boundary force. The analytic transfer energy is the difference between the solvation energy of a Born ion of radius 1.0 Å and a Born ion of radius 1.5 Å, both having 0.5 proton charges. The analytic result is 13.7 kcal/mol.

Calculations were performed for the same four positions and orientations with respect to the finite difference grid as in the previous tests. When the transfer works were calculated for the four different runs, the results range between 11.9 and 12.9 kcal/mol, in good agreement with the analytic result. The force balance in these calculations is excellent; that is, as required by Newton's third law of motion, the net force on the system is consistently small. The largest net force found in any of the calculations described in the previous paragraph is 0.71 kcal/(mol Å), and the average net force is closer to 0.3 kcal/(mol Å).

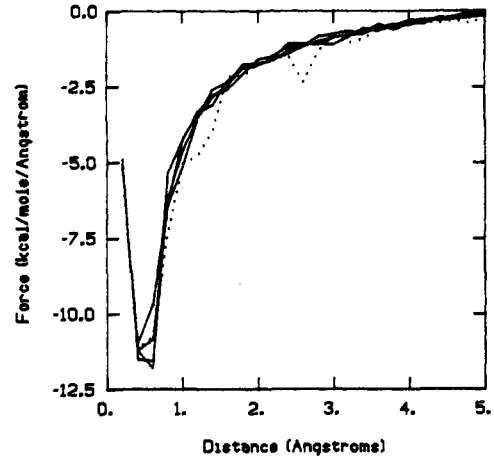

Figure 2. Graphs of force (kcal/(mol Å)) versus distance (Å) for a 1.0-Å dielectric cavity of charge 0.5 protons in the vicinity of a 1.5-Å cavity. Dots: virtual work forces. Solid lines: direct force calculations, for four different locations and orientations relative to the finite difference grid.

These calculations are further validated by comparison with "virtual work" forces computed for the neutral cavity. For each relative position of the two atoms, the neutral cavity was displaced by +0.02 and −0.02 Å along the axis joining the atoms, and an FDPB calculation was performed for each of the two positions, yielding an energy difference ΔG. The force on the cavity is then computed as $F = -\Delta G/0.04$ kcal/(mol Å). Figure 2 plots force versus distance between the two atoms as computed by this virtual work technique. The forces computed by the four runs described in this section are plotted as well, to permit comparison. (The plotted forces are actually the dot product of the computed force on the neutral cavity with the unit vector along the line connecting the two atoms.) The agreement is excellent for the most part, and the discrepancies at 2.6 and near 1.4 Å appear to result from numerical errors in the virtual work calculations, rather than in the rapid force calculations. Significant discrepancies are seen at about 0.5 Å, but this distance is very small compared to an actual bond length, and therefore the errors in this range should not arise in calculations on actual molecules. These results demonstrate that the forces along the axis joining the two atoms are accurate. It should also be noted that the force components off this axis are generally small. The largest off-axis force component found was 0.92 kcal/(mol Å), for the case of a net force of 4.6 kcal/(mol Å). The off-axis forces are more commonly on the order of 0.2 kcal/(mol Å).

3.1.4. Three Cavity Transfer Energy. The method used here for converting boundary forces into atomic forces is not rigorous for those surface regions which are defined by a probe contacting

TABLE III: Atomic Forces (kcal/(mol Å)) Due to Solvent on the Atoms of a Salt Bridge in Triose Phosphate Isomerase. Columns Present the *x*-, *y*-, and *z*-Force Components and the Force Magnitudes

(a) Results of Virtual Work Calculations

atom	F_x	F_y	F_z	|F|
Asp C_β	0.50	0.51	−0.50	0.87
Asp C_γ	3.00	−0.01	4.99	5.83
Asp $O_{\delta 1}$	−12.99	−2.50	−2.99	13.56
Asp $O_{\delta 2}$	−9.01	−11.00	−3.00	14.53
Asp net	−18.50	−13.00	−1.50	22.66
Lys C_ϵ	−1.49	2.49	1.00	3.07
Lys N_ζ	−4.49	−5.51	−2.00	7.38
Lys $H_{\zeta 1}$	7.51	1.01	0.01	7.58
Lys $H_{\zeta 2}$	7.01	8.51	1.50	11.12
Lys $H_{\zeta 2}$	10.50	6.49	1.99	12.50
Lys net	19.04	12.99	2.50	23.18
system net	0.54	−0.01	1.00	1.14

(b) Results of Direct Force Calculation Method, for Two Locations (Cases A and B) on the Finite Difference Grid

	case A				case B			
atom	F_x	F_y	F_z	|F|	F_x	F_y	F_z	|F|
Asp C_β	0.52	0.63	−0.27	0.86	0.55	0.60	−0.31	0.88
Asp C_γ	2.68	0.04	3.65	4.53	2.54	−0.06	3.62	4.42
Asp $O_{\delta 1}$	−12.99	−2.50	−3.44	13.67	−12.78	−2.66	−3.45	13.50
Asp $O_{\delta 2}$	−9.40	−11.91	−3.11	15.49	−9.41	−11.79	−3.10	15.40
Asp net	−19.19	−13.74	−3.17	23.81	−19.10	−13.91	−3.24	23.85
Lys C_ϵ	−0.34	1.79	1.81	2.57	−0.38	1.91	1.79	2.64
Lys N_ζ	−4.37	−5.33	−2.40	7.30	−4.37	−5.34	−2.40	7.31
Lys $H_{\zeta 1}$	7.36	1.62	0.62	7.57	7.34	1.74	0.56	7.57
Lys $H_{\zeta 2}$	6.66	8.34	0.87	10.71	6.72	8.40	0.99	10.81
Lys $H_{\zeta 2}$	9.97	7.19	2.34	12.51	9.98	7.26	2.30	12.55
Lys net	19.28	13.61	3.24	23.82	19.29	13.97	3.24	24.04
system net	0.09	−0.13	0.07	0.17	0.19	0.06	0.00	0.20

three or more atoms at the same time (see Methods). The present section describes a three-atom-transfer process involving such surface regions. A neutral 1.5-Å cavity is located at the origin, and a neutral 2.0-Å cavity is initially positioned at (0,−1.5,0). A 1.0-Å cavity having charge 0.5 protons begins at (5,0,0) and is moved to (0,0,0) in 0.2-Å steps. Then the 2-Å sphere is moved to (0,0,0) in 0.2-Å steps. The net result is that the charge is transferred from a 1.0-Å to a 2.0-Å cavity. The analytic energy difference is 20.5 kcal/mol. When the transfer work is obtained by force·distance for the translated cavities, using the methods described in this paper, the result is 19.0 kcal/mol. The excellent agreement implies that the treatment of the convex surface shared by the three atoms at a certain stage of the process is reasonably accurate.

3.2. Protein Salt Bridge: Force Analysis and Comparison with Virtual Work Forces. The final test case is that of the salt bridge between Lys 158 and Asp 155 of chicken triose phosphate isomerase. The distance between the Asp C_γ and the Lys N_ζ is 3.5 Å. To generate a small test system, the four side chain atoms of the Asp (net charge −1 proton), and the four Lys side chain atoms including and distal to C_ϵ (net charge +1 proton), were excised from the remainder of the protein and treated artificially as a nine-atom solute, immersed in water. Every atom in this system carries charge, and all but one have exposed probe accessible surface. Force calculations with the grid center at (38.4,25.3,−13.84), and (38.5,25.4,−13.83), (cases A and B) were performed to test the stability of the results with respect to grid position. (See Methods for further details.)

As described in Methods, the qE force on each atom can be separated into the sum of a reaction field force, due to the solvent, and the grid's version of the Coulomb's law force. To eliminate any inaccuracy which might result from the latter, the grid Coulombic forces were computed separately and subtracted from those of the FDPB runs. The resulting qE forces are those due to the solvent reaction field alone. Because the dielectric boundary forces are also due solely to the presence of solvent, the resulting force on each atom, computed in this way, is just that exerted by the solvent. There is no atom–atom Coulomb force.

For comparison, virtual work force calculations were performed. Each atom in turn was translated by +0.01 and then −0.01 Å in the *x*-, the *y*-, and the *z*-directions. The FDPB energy, G, was calculated for each translation. Then additional "reference" energies were computed with the entire grid set to the dielectric constant of the molecular interior. These reference energies were subtracted from the initial energies to yield charge–solvent interaction energies, G_{sol}. The force exerted *by the solvent* on each atom is calculated as $-\Delta G_{sol}/0.02$, where the ΔG_{sol} values are differences for +0.01- and −0.01-Å translations of each atom. These virtual work solvent forces are directly comparable with the solvent forces computed as the sum of qE and dielectric boundary forces, as described in the previous paragraph.

Table III present the results of the virtual work calculations, and of the two direct force calculations. The agreement among the tables is excellent. The largest discrepancy is for Lys C_ϵ, where the virtual work F_x differs from both rapid force results by about 1.1 kcal/(mol Å). Because the virtual work method is not exact, it is not certain which method is in error here. The net force on the system, which should be zero, is very small for both direct force calculations. The magnitudes of the net forces are 0.20 and 0.17 kcal/(mol Å).

Because this is a realistic test case, it is of interest to examine the salt bridge forces more closely. From Table IIIb, the net solvent force on the Asp is (−19.2,−13.7,−3.2) (in units of kcal/(mol Å)), and the net solvent force on the Lys is equal and opposite. (This force balance is required by the need for the net force to be zero, together with the fact that the only additional force term, the Coulombic term, also nets to zero.) The net solvent force tends to separate the two side chains. However, when analytic Coulomb's law forces are added back, the total force on the Asp is (5.2,4.9,−0.2), and again the Lys force is equal and opposite. This total electrostatic force acts to push the two groups together, as expected for a salt bridge. When dielectric boundary

forces are neglected, the only remaining atomic forces are the qE forces, which are the sum of the Coulomb's law and reaction field forces. This net qE force on the Asp is (8.9,8.2,-3.8), while the net qE force on the Lys is (-8.4,-1.8,3.3). Thus, the net qE force is (0.5,6.4,-0.6). This is clearly *not* equal to zero. As noted in the Introduction, there is no guarantee that the net qE force will equal zero in a system described by the PBE. Force balance will be obtained in general only if the dielectric boundary forces are included.

4. Discussion

As derived in the Methods section, the electrostatic forces in a system governed by the PBE may be separated into three components: qE forces, resulting from the action of the electric field on "fixed" charges; dielectric boundary forces, which always act as a pressure on dielectric boundaries, directed into the lower dielectric region; and ionic boundary forces, which also represent a pure pressure. The qE forces, in turn, may be expressed as the sum of Coulombic forces and reaction field forces. The net effect of solvent, then is the sum of reaction field forces, dielectric boundary forces, and ionic forces. However, the ionic forces should be negligibly small in most calculations in which dielectric boundaries are present.

In contrast, the dielectric boundary forces are far from negligible. There is no reason to expect that calculated forces on atoms which form part of a dielectric boundary will be accurate if this force contribution is neglected. In fact, neglecting boundary forces will lead to a nonzero net force on the system, as described above.

The fact that Coulombic forces may be separated from reaction field forces has already been exploited in a molecular dynamics simulation using the FDPB method.[6] Coulombic forces were updated as usual in this simulation, but the reaction field force was recalculated only every N steps of the simulation. It should be clear that the same procedure can be used for the dielectric boundary forces. Thus, a molecular dynamics simulation may update Coulombic forces as usual, while the net solvent force on each atom—the sum of the reaction field force and the dielectric boundary force—may be recalculated only every N steps. As previously noted,[6] such a procedure is physically justified by the fact that the dielectric relaxation time of water is much greater than the standard molecular dynamics time step. The incorporation of an FDPB calculation in a molecular simulation also raises the possibility that long-range Coulombic interactions may be included via the grid solution, without the need for a Coulombic interaction cutoff. Such an approach would resemble the particle–particle and particle–mesh method for treating ionic liquids.[42]

The computer time for the calculations presented here is dominated by the process of generating the dielectric maps and then solving the PBE on the finite difference grid. The force calculations themselves are quite rapid. For example, setting up and executing the FDPB calculation for the 9-atom triose phosphate isomerase salt bridge calculation here requires about 30 CPU seconds on a CRAY YMP, but the force calculations require less than 1 s. Much of the 30 s is spent in generating an accurate dielectric map, because many probe spheres are required. Optimization of this segment of code should yield significant acceleration.

One potentially significant limitation of the present method has to do with the probe-accessible surface definition. Consider the case of a large molecule containing a cavity just large enough to accommodate a single solvent probe. Such a cavity will be set to the dielectric constant of the solvent in the standard implementation of the PBE method. In this special case, it is possible that the entire cavity will be obliterated by an infinitesmal atomic displacement. Because changing the cavity permittivity suddenly from ϵ_s to ϵ_l produces a discontinuous energy change, the force on atoms bounding the cavity is infinite. This may not be entirely nonphysical, given that measurements of forces between two mica plates separated by a thin layer of water show sharp force variations on the size scale of a water molecule.[43] On the other hand, some practical method of dealing with such cases is needed. In the present method, no sharp force increase will be observed in such a case, because the method is capable of treating only small distortions in an existing boundary; not the sudden appearance or disappearance of an entire boundary surface. The boundary element technique will perform similarly. It should be possible to devise algorithms which will tie atomic movements to dielectric constant changes in such cavities and therefore provide reasonable forces. For now, however, it would seem that caution should be used in treating systems containing many atoms, where this problem may arise. Note that this problem is not limited to the calculation of electrostatic forces: any energy term which depends upon the probe-accessible surface will have discontinuous derivatives with respect to atomic positions. Ultimately, the best solution may be to use a different definition of the surface.

Another limitation of the method is that it yields relatively inaccurate dielectric boundary forces for cavities which contain no charges (see section 3.1.1). This appears to be related to the fact that in such cases, the electrostatic field at the boundary tends to run tangent to the boundary. In contrast, the field produced by an internal charge will be nearly perpendicular to the boundary. Improved methods for treating such cases are under development. For now, however, given that the dielectric boundary forces produced by internal charges are much stronger than those produced by external charges, the method should work well in most molecular simulations. It should be used cautiously, however, in computing the effects of external fields on molecules in solution.

In conclusion, the methods presented here should make it possible to begin incorporating the predictions of the PBE rigorously into molecular mechanics simulations. For now, the limits of computational time and the problem of cavities in the probe-accessible surface are likely to limit the range of applicability to systems containing a modest number of atoms. It will be of interest to examine the predictions of this approach for the conformational preferences of hydrated molecules. This method should also be of help in predicting reaction coordinates for small solvated systems. Such studies are now under way. With further development of the algorithms, it should be possible to use these methods to study larger, biomolecular systems, such as proteins, nucleic acids, and lipid bilayers.

Acknowledgment. We are grateful to Dr. B. Bush for his comments on the probe-accessible surface and to Drs. H. S. R. Gilson, T. Truong, and M. Zacharias for stimulating discussions. This work was supported in part by the NIH, the Robert A. Welch Foundation, ONR, and the Illinois Supercomputer Center. M.K.G. is a Howard Hughes Medical Institute Physician Research Fellow. B.A.L. is the recipient of an NIH Predoctoral Traineeship in the Houston Area Molecular Biophysics Program. J.A.M. is the recipient of the G. H. Hitchings Award from the Burroughs Wellcome Fund.

References and Notes

(1) Harvey, S. C. *Proteins* **1989**, *5*, 78.
(2) Davis, M. E.; McCammon, J. A. *Chem. Rev.* **1990**, *90*, 509.
(3) Sharp, K.; Honig, B. *Annu. Rev. Biophys. Biophys. Chem.* **1990**, *19*, 301.
(4) Davis, M. E.; McCammon, J. A. *J. Comput. Chem.* **1990**, *11*, 401.
(5) Sharp, K. *J. Comput. Chem.* **1991**, *12*, 454.
(6) Niedermeier, C.; Schulten, K. *Mol. Simulation* **1992**, *8*, 361.
(7) Zauhar, R. J.; Morgan, R. S. *J. Mol. Biol.* **1985**, *186*, 815.
(8) Rashin, A. A. *J. Phys. Chem.* **1989**, *93*, 4664.
(9) Juffer, A. H.; Botta, E. F. F.; van Keulen, B. A. M.; van der Ploeg, A.; Berendsen, H. J. C. *J. Comput. Phys.* **1991**, *97*, 144.
(10) Vorobjev, Y. N.; Grant, J. A.; Scheraga, H. A. *J. Am. Chem. Soc.* **1992**, *114*, 3189.
(11) Yoon, B. J.; Lenhoff, A. M. *J. Phys. Chem.* **1992**, *96*, 3130.
(12) Zauhar, R. J. *J. Comput. Chem.* **1991**, *12*, 575.

(13) Richards, F. M. *Annu. Rev. Biophys. Bioeng.* **1977**, *6*, 151.
(14) Still, W. C.; Tempczyk, A.; Hawley, R. C.; Hendrickson, T. *J. Am. Chem. Soc.* **1990**, *112*, 6127.
(15) Schaefer, M.; Froemmel, C. *J. Mol. Biol.* **1990**, *216*, 1045.
(16) Gilson, M. K.; Honig, B. *J. Computer-Aided Mol. Design* **1991**, *5*, 5.
(17) Whitlow, M.; Teeter, M. M. *J. Am. Chem. Soc.* **1986**, *108*, 7163.
(18) Pickersgill, R. W. *Protein Eng.* **1988**, *2*, 247.
(19) Conway, B. E.; Bockris, J. O.; Ammar, I. A. *Trans. Faraday Soc.* **1951**, *47*, 756.
(20) Mehler, E. L.; Eichele, G. *Biochemistry* **1984**, *23*, 3887.
(21) Warshel, A.; Russel, S. T.; Churg, A. K. *Proc. Natl. Acad. Sci. U.S.A.* **1984**, *81*, 4785.
(22) Sharp, K. A.; Honig, B. *J. Phys. Chem.* **1990**, *94*, 7684.
(23) Reiner, E. S.; Radke, C. J. *J. Chem. Soc., Faraday Trans.* **1990**, *86*, 3901.
(24) Henderson, D.; Blum, L.; Lebowitz, J. L. *J. Electroanal. Chem.* **1979**, *102*, 315.
(25) Verwey, E. J. W.; Overbeek, J. Th. G. *Theory of the Stability of Lyophobic Colloids*; Elsevier: New York, 1948.
(26) Becker, R. *Electromagnetic Fields and Interactions*; Blackie and Son: London, 1964.
(27) Stratton, J. A. *Electromagnetic Theory*; McGraw-Hill: New York, 1941.
(28) Henderson, D.; Blum, L. *J. Chem. Phys.* **1978**, *69*, 5441.
(29) Henderson, D.; Blum, L.; Lebowitz, J. L. *J. Electroanal. Chem.* **1979**, *102*, 315.
(30) Luty, B. A.; Davis, M. E.; McCammon, J. A. *J. Comput. Chem.* **1992**, *13*, 768.
(31) Luty, B. A.; Gilson, M. K.; Davis, M. E.; McCammon, J. A., unpublished results.
(32) Davis, M. E.; McCammon, J. A. *J. Comput. Chem.* **1991**, *12*, 909.
(33) Gilson, M. K.; Sharp, K. A.; Honig, B. H. *J. Comput. Chem.* **1987**, *9*, 327.
(34) Lee, B.; Richards, F. M. *J. Mol. Biol.* **1971**, *55*, 379.
(35) Davis, M. E.; Madura, J. D.; Luty, B. A.; McCammon, J. A. *Comput. Phys. Commun.* **1991**, *62*, 187.
(36) Bernstein, F. C.; Koetzle, T. F.; Williams, G. J. B.; Meyer, E. F., Jr.; Brice, M. D.; Rodgers, J. R.; Kennard, O.; Shimanouchi, T.; Tasumi, M. J. *J. Mol. Biol.* **1977**, *112*, 535.
(37) Banner, D. W.; Bloomer, A. C.; Petsko, G. A.; Phillips, D. C.; Wilson, I. A. *Biochem. Biophys. Res. Commun.* **1976**, *72*, 146.
(38) Brooks, B. R.; Bruccoleri, R. E.; Olafson, B. D.; States, D. J.; Swaminathan, S.; Karplus, M. *J. Comput. Chem.* **1983**, *4*, 187.
(39) Jorgensen, W. L.; Tirado-Rives, J. *J. Am. Chem. Soc.* **1988**, *110*, 1657.
(40) Jarvis, L.; Huang, C.; Ferrin, T.; Langridge, R. UCSF MIDAS User's Manual, 1986.
(41) Kirkwood, J. G. *J. Chem. Phys.* **1934**, *2*, 351.
(42) Eastwood, J. W.; Hockney, R. W.; Lawrence, D. *Comput. Phys. Commun.* **1980**, *19*, 215.
(43) Israelachvili, J. N. *Acc. Chem. Res.* **1987**, *20*, 415.